

Article

Evaluation of Goethite as a Catalyst for the Thermal Stage of the Westinghouse Process for Hydrogen Production

Carmen M. Fernández-Marchante, Alexandra Raschitor, Ismael F. Mena , Manuel A. Rodrigo  and Justo Lobato * 

Chemical Engineering Department, Enrique Costa Novella Building, Av. Camilo Jose Cela n 12, University of Castilla-La Mancha, 13004 Ciudad Real, Spain; carmenm.fmarchante@uclm.es (C.M.F.-M.); alexandra.raschitor@uclm.es (A.R.); Ismael.fernandez@uclm.es (I.F.M.); Manuel.Rodrigo@uclm.es (M.A.R.)

* Correspondence: justo.lobato@uclm.es; Tel.: +34-926-295-300

Abstract: This work focuses on the evaluation of goethite as a catalyst for the transformation of sulfuric acid into sulfur dioxide, a reaction with great interest for the hybrid electrochemical-thermoelectrochemical Westinghouse cycle for hydrogen production. A comparison of the performance of goethite with that of CuO, Fe₂O₃, and SiC has been carried out. Moreover, a mixture of those catalysts was evaluated. The results demonstrate that goethite can be used as a catalyst for the thermal decomposition of sulfuric acid in the Westinghouse cycle, with an activity higher than that of SiC but lower than that of Fe₂O₃ and CuO. However, it does not undergo sintering during its use, but just produces small particles in its surface, which remain after the treatment. Mixtures of Fe₂O₃ with SiC or goethite do not produce synergism, thus operating each catalyst in an independent way.



Citation: Fernández-Marchante, C.M.; Raschitor, A.; Mena, I.F.; Rodrigo, M.A.; Lobato, J. Evaluation of Goethite as a Catalyst for the Thermal Stage of the Westinghouse Process for Hydrogen Production. *Catalysts* **2021**, *11*, 1145. <https://doi.org/10.3390/catal11101145>

Academic Editors: Vincenzo Baglio, Carlo Santoro, David Sebastián, Minhua Shao and Yingze Song

Received: 19 August 2021

Accepted: 21 September 2021

Published: 24 September 2021

Publisher's Note: MDPI stays neutral with regard to jurisdictional claims in published maps and institutional affiliations.



Copyright: © 2021 by the authors. Licensee MDPI, Basel, Switzerland. This article is an open access article distributed under the terms and conditions of the Creative Commons Attribution (CC BY) license (<https://creativecommons.org/licenses/by/4.0/>).

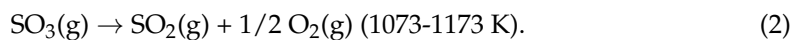
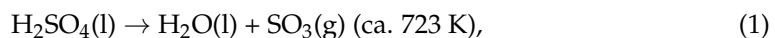
1. Introduction

One of the challenges facing today's society is the use of cleaner energy sources. In this context, hydrogen is considered as an interesting alternative to traditional fuels, involving technologies that have associated low or even zero emissions.

Nowadays, storage of energy as hydrogen is considered as a plausible challenge, which will help in optimizing the management of energy using renewable sources. This may have an important impact in windmill and solar photovoltaics, which are known to be easily coupled with electrolyzers for the production of hydrogen.

In addition to the electrochemical methods, hydrogen can also be produced by different technologies such as thermal, photocatalytic, biological or photonic processes [1]. In this context, water splitting using photoelectrochemical, thermochemical or hybrid thermoelectrochemical cycles are currently hot research topics [2]. It is worth highlighting that the hybrid sulfur cycle or Westinghouse cycle, consists of a hybrid electrochemical-thermochemical process proposed by the Westinghouse electric corporation in 1975 [3]. Among the over 100 proposed processes to produce hydrogen, the Westinghouse cycle was selected as one of the final options using refined criteria [4,5].

Figure 1 shows a scheme of this cycle. As can be seen, it consists of two main steps. First, the sulfuric acid is thermally decomposed in two successive reactions. In the first reaction, sulfuric acid is decomposed into water and sulfur trioxide (Equation (1)). Thereafter, sulfur trioxide is catalytically decomposed into oxygen and sulfur dioxide (Equation (2)) [6,7]. This process requires a high input of energy that can be driven by the concentrated solar power [8].



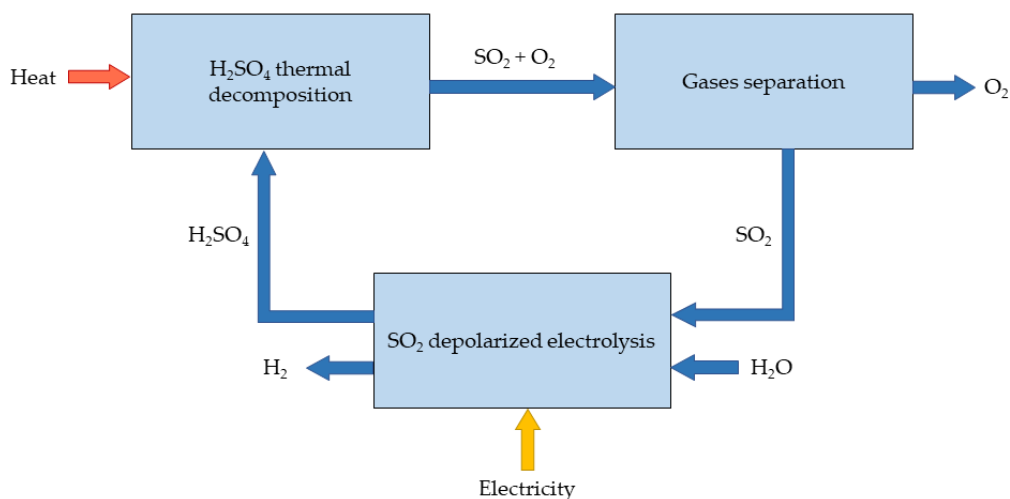
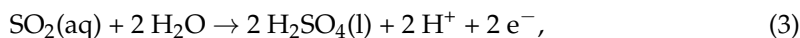


Figure 1. Westinghouse cycle scheme.

Following this step, SO_2 is separated from O_2 and introduced in an electrochemical cell. SO_2 is then oxidized into sulfuric acid, protons, and electrons at the anode (Equation (3)). The protons are recombined with electrons on the cathode to form hydrogen (Equation (4)). The overall cell voltage is more than 7 times lower than that needed in the conventional electrochemical splitting of water. Therefore, this process requires a lower voltage (0.158 V vs. SHE) than the direct electrolysis of water (1.23 vs. SHE) for hydrogen production [9]. This electrochemical cell can be operated with photovoltaic panels as the typical water electrolysis. Therefore, similar to other thermochemical processes, hydrogen and oxygen are the only outputs, and the acid by-products are not expelled. Moreover, the hybrid cycle has the following advantages: (a) It requires lower temperatures; and (b) can be driven by the concentrated and photovoltaic solar power energy. Energy efficiencies of around 50% have been reported [8].



One of the key points of the process is the fact that the catalyst is used for the sulfuric acid decomposition [10]. The efforts are focused on the development of the catalyst, that can offer high activity and stability in the process, with the lowest cost possible.

Up to now, most of the studied catalysts are based on noble metals (Pt, Pd, Rh, Ir, Ru) supported on different materials (Al_2O_3 , ZrO_2 , TiO_2 , SiC) [11–14]. These metals are active for the sulfuric acid decomposition and present high resistance to the acidic corrosion [2]. Nevertheless, they can suffer metal loss or sintering at high temperature [15,16]. Rashkeev et al. (2009) compared the use of different noble metals as catalysts, obtaining as the best result, a SO_2 production rate of around 1 mol/g_{cat}/h using Pt (weight hourly space velocity (WHSV): 230 g H_2SO_4 /g_{cat}/h, 1123 K). This production was reduced until 0.4 mol/g_{cat}/h for the Pd catalyst and less than 0.1 mol/g_{cat}/h for Rh, Ir, and Ru [12]. Regarding the supporting material, Ginosar et al. (2007) stated that Pt supported on Al_2O_3 and ZrO_2 catalysts presented higher activities than on TiO_2 at 1073–1123 K (WHSV: 52 g H_2SO_4 /g_{cat}/h) [17]. Pt supported on the silicon carbide (SiC) catalyst has also been evaluated, presenting high activity (60% at 1123 K at a gas hourly space velocity (GHSV) of 72,000 mL/g_{cat}/h (corresponding to a WHSV of 157.5 g H_2SO_4 /g_{cat}/h) using N_2 as a carrier gas) and stability (360 min) in the H_2SO_4 decomposition [11,18].

A cheaper alternative to the use of noble metals comes from the use of different metal oxides. Therefore, several metal oxides have emerged as cheap, available, and active catalysts for the sulfuric acid decomposition [19]. Tagawa and Endo (1989) studied different metal oxides and established the following order of catalysts, regarding their activity in

sulfuric acid decomposition: $\text{Cr}_2\text{O}_3 > \text{Fe}_2\text{O}_3 > \text{CuO} > \text{CeO}_2 > \text{NiO} > \text{Al}_2\text{O}_3$ (4.0 mol% of SO_3 using N_2 as a carrier gas, 873–1173 K) [20]. With the objective of improving their activity, Ginosar et al. (2009) evaluated the sulfuric acid decomposition in long term experiments (≈ 160 h) using different complex metal oxides as catalysts, obtaining the following order: $2\text{CuO}\cdot\text{Cr}_2\text{O}_3 > \text{CuFe}_2\text{O}_4 > \text{NiCr}_2\text{O}_4 \approx \text{NiFe}_2\text{O}_4 > \text{MnTiO}_3 \approx \text{FeTiO}_3$ (WHSV: ≈ 2000 g $\text{H}_2\text{SO}_4/\text{g}_{\text{cat}}/\text{h}$, 1123 K) [21]. Chromite catalysts suffered from leaching of chromium, obtaining NiO and $\text{Cu}_2\text{O}/\text{CuO}$ as the remaining samples. In the case of CuFe_2O_4 catalyst, the material was decomposed into CuO and Fe_2O_3 in the first 72 h, in which the activity remains associated with the CuO . From these results, it is evident that the best activity was obtained by CuO , with the accompanied Cr and Fe oxides typically leached or deactivated.

Iron oxides have always been seen as the most interesting alternative, due to their low cost and extremely promising results. Nadar et al. (2018) obtained the following activity order using different iron oxide-supported catalysts: $\text{Fe}_2\text{O}_3/\text{SiO}_2 > \text{Fe}_2\text{O}_3/\text{TiO}_2 > \text{Fe}_2\text{O}_3/\text{ZrO}_2 > \text{Fe}_2\text{O}_3/\text{CeO}_2$ (WHSV: 27 g $\text{H}_2\text{SO}_4/\text{g}_{\text{cat}}/\text{h}$, 1073 K) [22]. However, there is still room for further developments, since the iron oxide chemistry is very interesting and iron can be found in different species.

Considering this background, in this work, goethite has been evaluated as a catalyst for sulfuric acid thermal decomposition. Goethite is a cheap material, naturally stable mineral, and widespread iron oxide [23–25]. It consists of an iron (III) oxide-hydroxide ($\alpha\text{-FeO(OH)}$) found as a sediment in nature. In this work, its performance is going to be compared with that of CuO and Fe_2O_3 , which have been selected as reference catalysts. Additionally, the performance of goethite will be compared with SiC , which has been employed as a stable and not catalytic material for H_2SO_4 decomposition. Moreover, a mixture of Fe_2O_3 with SiC and goethite have been used to determine the possible synergistic effect on the catalytic activity.

2. Results and Discussion

Figure 2 shows the time course of the total SO_2 production, during a test carried out at 1173 K with 1 g of CuO as the catalyst and WHSV of 50 g $\text{H}_2\text{SO}_4/\text{g}_{\text{cat}}/\text{h}$ (calculated as the amount of the evaporated sulfuric acid divided by the catalyst amount and the time of reaction). As can be seen, the catalytic reactor can efficiently generate SO_2 . It is worth highlighting that the total SO_2 was measured as the sum of the SO_2 retained in the NaOH trap as Na_2SO_3 . Additionally, the SO_2 condensed along with the water and H_2SO_4 . Moreover, most of the SO_2 formed passed in a gaseous form through the condenser and, finally, it was bubbled into the NaOH solution. Therefore, only an amount of 7 mmol of SO_2 was condensed with the acidic solution, corresponding to 1.14% of the total SO_2 formed.

The H_2SO_4 conversion to SO_2 is affected by the temperature and the amount of catalyst, as shown in Figure 3 (calculated as mmol of SO_2 measured per mmol of the evaporated sulfuric acid). Regarding the temperature, using 5 g of CuO , the conversion increased from 37 to 47% when the temperature increased 50 K, from 1123 to 1173 K. As expected, the use of higher temperatures favored the SO_2 formation [21]. Regarding the amount of catalyst, an increase from 1 to 10 g of CuO produced an increase in the H_2SO_4 conversion from 44 to 59%. These values are far from the desired 100%, suggesting that sulfuric acid could bypass the catalytic bed without a reaction. Nevertheless, these conversions are similar to that obtained by Noh et al. (2014) using a Pt/SiC catalyst [11]. It is evident here that the use of the higher amount of catalyst favored the transformation of H_2SO_4 into SO_2 . However, this increase was not proportional to the amount of catalyst added, reducing the efficiency of the process in terms of the net use of the catalyst, most likely due to the fact that it is near the reachable maximum values. From these results, the use of 1 g of the catalyst at 1173 K were established as the operation conditions for the following experiments.

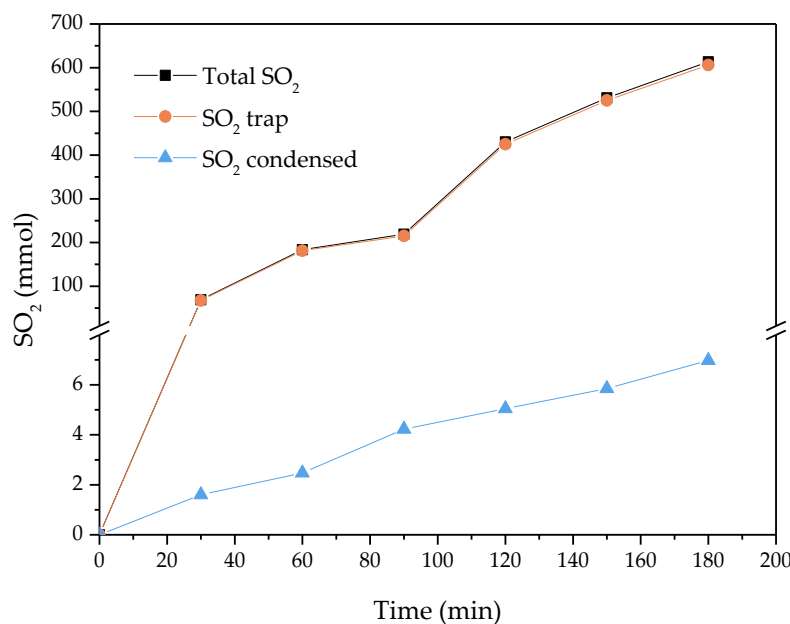


Figure 2. The SO₂ amount produced in the catalytic decomposition of H₂SO₄ using 1 g of CuO at 1173 K.

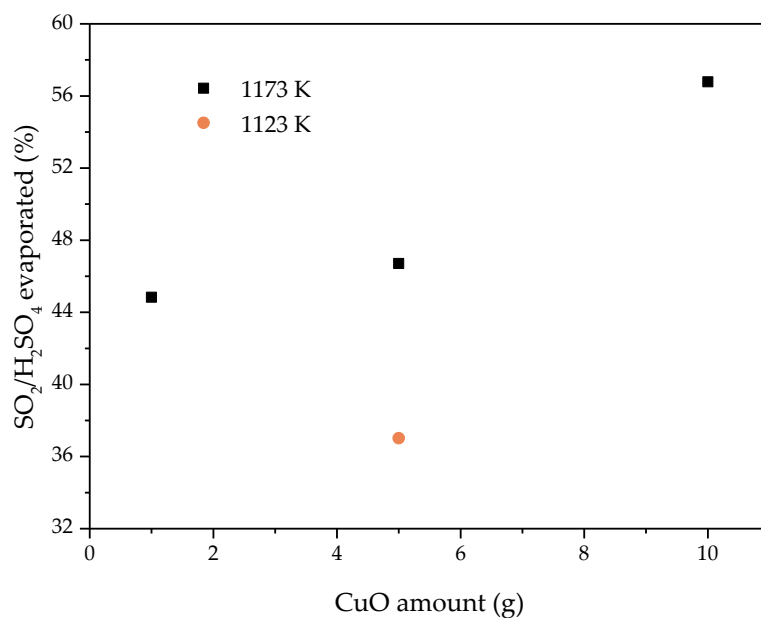


Figure 3. Influence of the temperature and catalysts amount in the H₂SO₄ conversion to SO₂.

Figure 4 compares the H₂SO₄ conversion to SO₂ obtained by different catalysts. The following sequence, in decreasing order of their activity, was obtained: Fe₂O₃ > CuO > Goethite > SiC. The pure metal oxides (Fe₂O₃ and CuO) produced the highest SO₂ conversion (49% at 90 min and 47% at 120 min, respectively). These results agree with those reported by Tagawa et al. (1989), which settled that the iron oxide presents higher activity than the copper oxide [20]. SiC reached the lowest activity of all the materials studied ($\approx 20\%$). In the case of the goethite, the activity obtained (36% at 120 min) was lower than that obtained for the Fe₂O₃, despite also being an iron hydroxide.

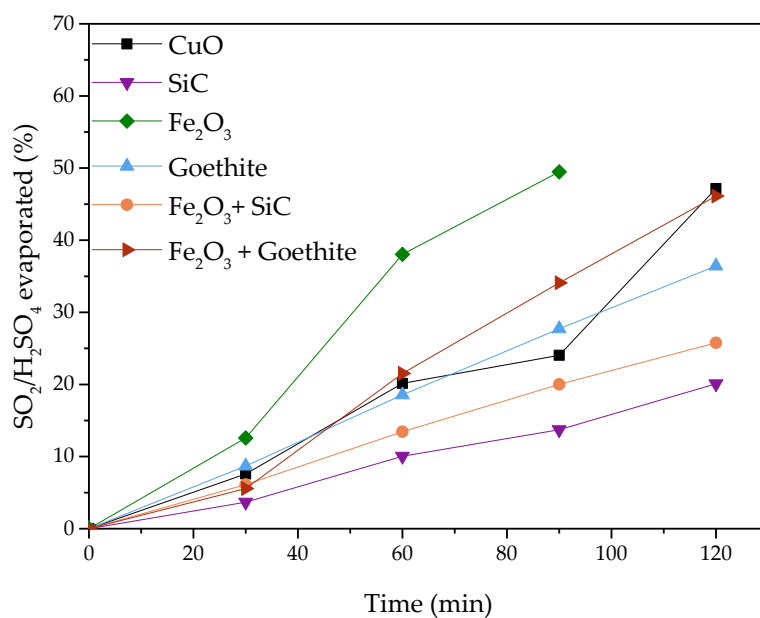


Figure 4. Time course of H_2SO_4 conversion to SO_2 by different catalysts (catalyst amount: 1 g; 1173 K).

Additionally, two experiments mixing Fe_2O_3 with SiC and goethite were carried out. The use of the mixture $\text{Fe}_2\text{O}_3 + \text{SiC}$ as a catalyst (0.5 g of each catalyst) produced an increase in the activity (26%), as compared with the pure SiC. Nevertheless, the conversion was considerably reduced as compared with the Fe_2O_3 , being one of the experiments that presented a low activity. Moreover, this conversion points out that the effect of the different catalysts is additive and there are no synergisms. Regarding the experiment carried out with a mixture of 0.5 g of Fe_2O_3 and 0.5 g of goethite as catalyst, it reached an intermediate conversion with respect to the pure materials (46%). This fact indicates again that there is no synergic effect between both materials, but just an intermediate behavior suggesting that each catalyst operated in an independent way regarding the other. The results obtained by goethite are very interesting, since this species overcomes the other catalysts and, as it will be shown and discussed in a later section of this manuscript, seems to be more stable against agglomeration.

Figure 5 shows the efficiency of the different catalysts studied in mmol of SO_2 produced per gram of H_2SO_4 evaporated and per gram of catalyst. Since the mmol of SO_2 were measured by the titration methods explained in the Experimental Methods section, the gram of sulfuric acid calculated by the difference between the initial and final weight and the gram of catalyst is the amount of weight introduced in the reactor. The lowest efficiencies obtained corresponded to the experiments using SiC, confirming its low activity in the SO_2 formation. Fe_2O_3 , $\text{Fe}_2\text{O}_3 + \text{goethite}$, CuO, and goethite obtained efficiency values 2.6, 2.4, 2.2, and 2.0 times higher than that obtained for the SiC, respectively. From these results, it is evident that the metal oxides presented a very high activity in the sulfuric acid decomposition, with Fe_2O_3 being the most active of the studied catalysts. Furthermore, this oxide and goethite mixture is very promising.

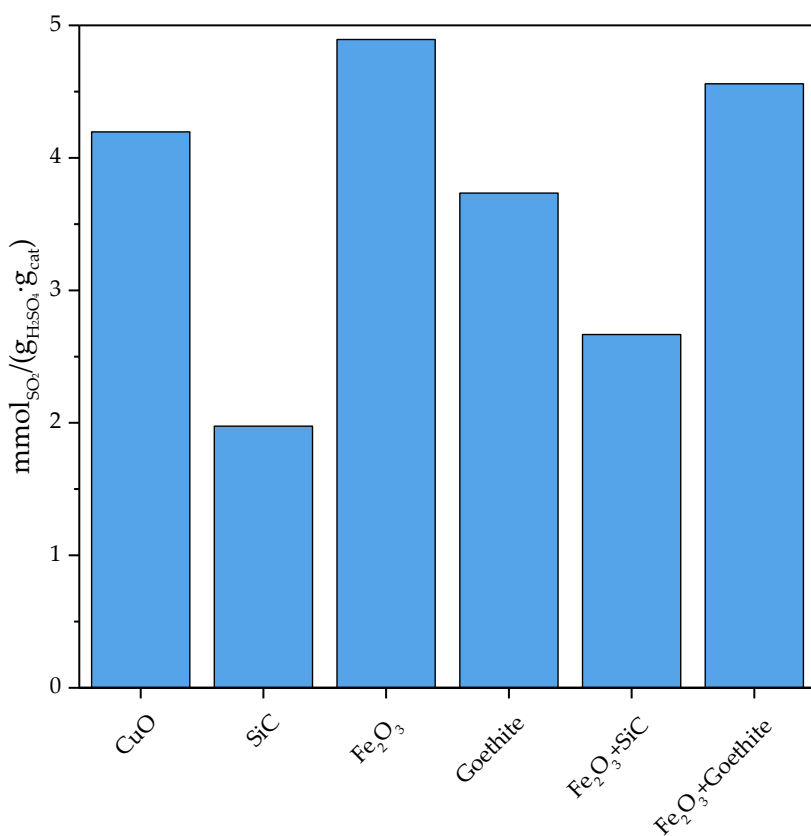


Figure 5. Total SO₂ efficiency of the catalysts studied (catalyst amount: 1 g; 1173 K).

The characterization of initial and final catalysts of the Fe₂O₃ as well as the goethite experiments were evaluated to determine the differences shown in their activities. Considering the Pourbaix diagram of iron, Fe²⁺ is the main species at acidic pH and 298 K in the water system. For that reason, the catalyst could suffer iron leaching during the process [26]. Therefore, the catalysts were characterized by the XRD analysis to determine the iron species, as shown in Figure 6. In the case of Fe₂O₃, the catalysts presented the same peaks before and after the reaction. These results indicate that the catalyst had the same crystalline phase at the end of the reaction, specifically, that of hematite form. Regarding the goethite, the initial sample presented a relatively amorphous form. However, after 2 h of reaction, the goethite was transformed due to the reaction conditions (mainly, the high temperature and its possible reaction with steam). After the reaction, goethite presented a similar crystallinity to the Fe₂O₃ sample (hematite).

Regarding the SEM images in Figure 7, both of the catalysts changed their surface. As can be seen in Figure 7a, the Fe₂O₃ presented a homogeneous granular surface. During the thermal decomposition of sulfuric acid, the catalyst suffered a sintering process in which the particles were agglomerated (Figure 7c), reducing the surface area available for the reaction. This sintering can cause a deactivation of the Fe₂O₃ in the long term use. In the case of goethite, the original catalyst presented a flat surface. After the reaction, it was transformed into a granular surface, similar to the initial Fe₂O₃. This result, together with the XRD analysis, seems to indicate that goethite was transformed into iron (III) oxide. In this case, the surface area of the catalyst is very similar (2.9 vs. 2.5 m²/g), in which the different sizes of the granules observed in the SEM may indicate a different distribution of micro and mesopores. These results are extremely promising since the reaction time was long enough to make this comparison. However, in the future, long term experiments should be carried out to further know the stability of goethite in its use as a catalyst of the Westinghouse process.

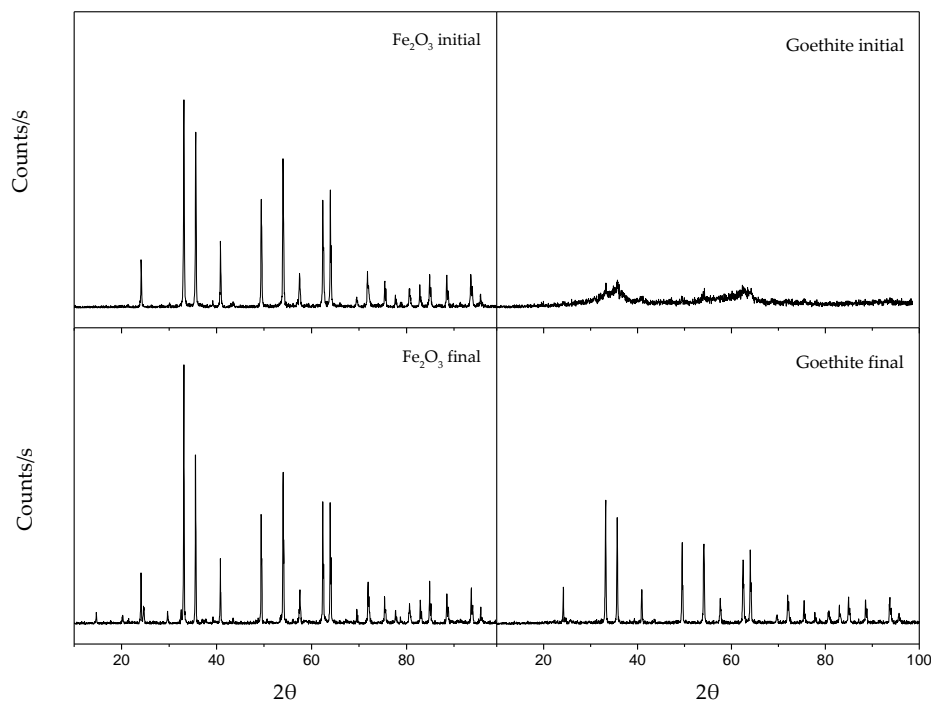


Figure 6. XRD of the initial and final Fe_2O_3 and goethite.

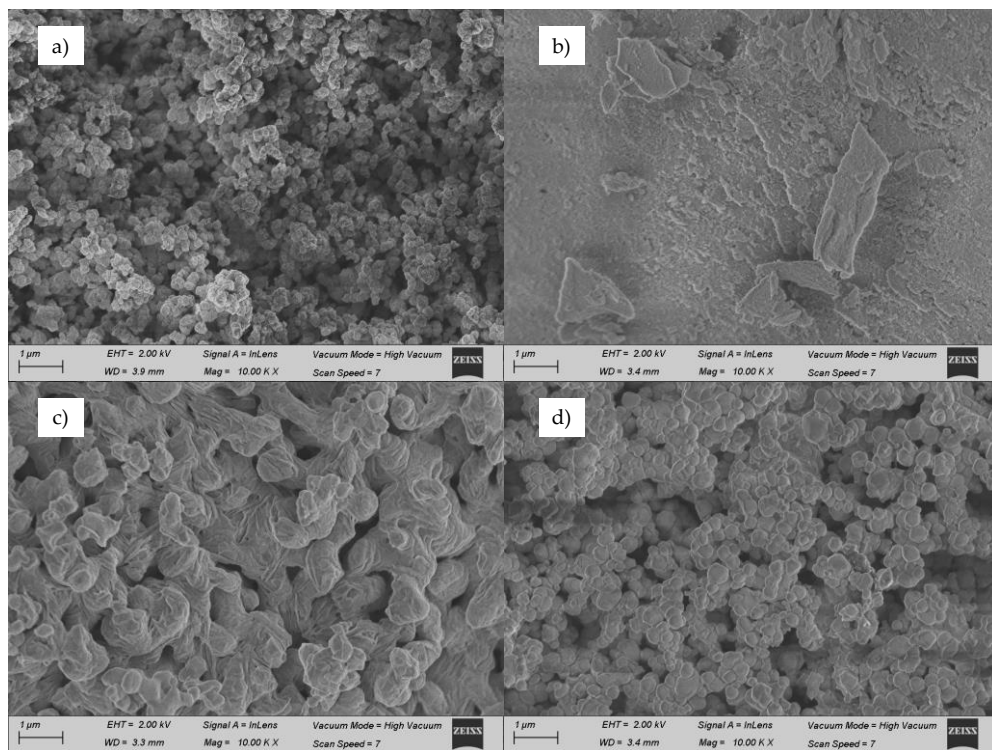


Figure 7. SEM images of initial (a,b) and final (c,d) Fe_2O_3 and goethite catalysts, respectively.

As can be seen, Figure 8 shows the EDX analysis and Table 1 presents the atomic percentage of O, Fe, and S of the initial and final catalysts. In both cases, the catalysts increased their content of sulfur and oxygen after the reaction. This fact can be related to the adsorption or the deposition of sulfuric acid, as well as the intermediates formed in the reaction. Regarding the inserted images, the sulfur appeared as distributed in the whole surface (blue color).

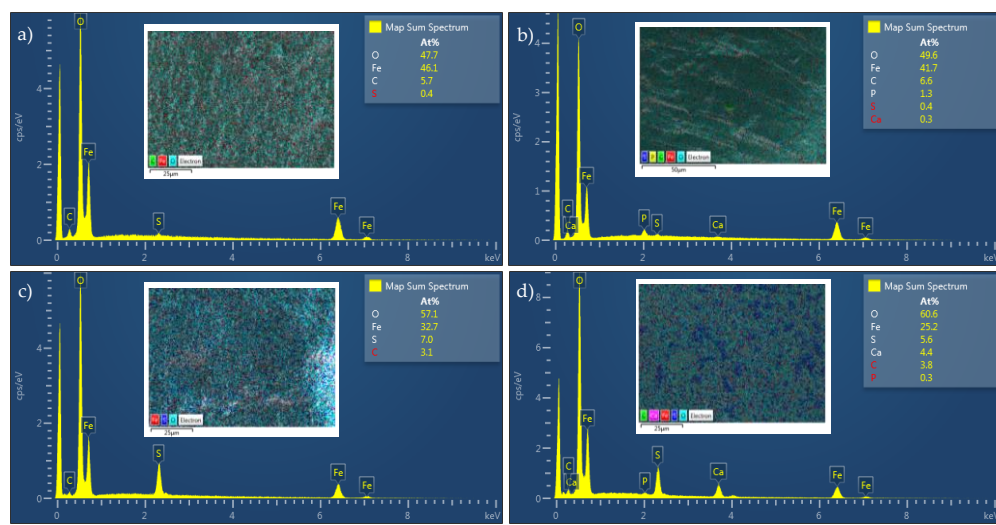


Figure 8. EDX analysis of initial (**a,b**) and final (**c,d**) Fe_2O_3 and goethite catalysts, respectively.

Table 1. EDX composition of the initial and final catalysts.

	Fe_2O_3 Initial/Final	Goethite Initial/Final
O (At%)	47.7/57.1	49.6/60.6
Fe (At%)	46.1/32.7	41.7/25.2
S (At%)	0.4/7.0	0.4/5.6

Finally, the Fourier transform infrared spectroscopy was carried out to monitor the chemical and structural changes in the goethite catalyst. A comparison of the FTIR spectra of the initial and final goethite samples is shown in Figure 9. As can be seen, the initial goethite presents vibration bands of the hydroxyl groups and/or water molecules at around 3400 and 1632 cm^{-1} [27]. These bands appear with a lower intensity in the final sample, indicating that the chemical surface of the goethite changed after the reaction, removing the water and hydroxyl groups. Moreover, in the initial sample, a very weak characteristic goethite band appears at 1380 cm^{-1} [27], which disappears in the sample after the reaction. Whereas, the final sample has a peak at 580 cm^{-1} associated with a Fe–O vibration band [22], which did not appear in the pristine sample. These results agree with those obtained in XRD, which indicated that the goethite surface was transformed into iron oxide.

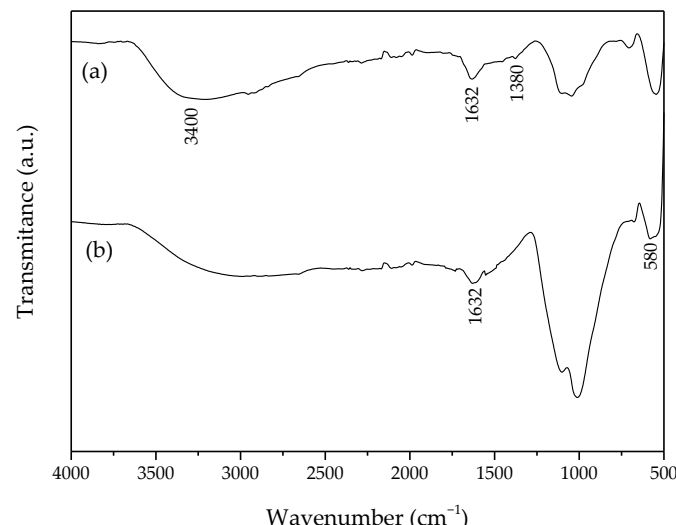


Figure 9. FTIR analysis of initial (**a**) and final (**b**) goethite catalysts.

3. Materials and Methods

Sulfuric acid (95–97%) was purchased from Scharlau (Sentmenat, Spain), as well as sodium hydroxide pellets and the phenolphthalein solution (1%) were obtained from Panreac (Castellar del Vallès, Spain). Copper (II) oxide (CuO , >99%, Merck, Darmstadt, Germany), iron (III) oxide (Fe_2O_3 , >96%, Sigma-Aldrich (Steinheim, Germany)), goethite ($\text{Fe(OH)}_2\text{O}$), iron (III) oxide hydrated, catalyst grade, Sigma-Aldrich), and silicon carbide (SiC , SICAT (Willstätt, Germany), extrudates 1 mm) were used as catalysts.

Figure 10 shows a scheme of the experimental setup used in the sulfuric acid decomposition. Sulfuric acid (100 mL) was introduced and boiled in a Florence Flask. The acid vapor was heated until 423–673 K and then led to a flow through the quartz reactor (length: 60 cm, diameter: 1 cm), in which a crushed catalyst bed was placed (bed diameter: 0.8 cm, 1–10 g). The catalytic reaction was carried out at 1123–1173 K inside a controlled furnace. The thermocouple was introduced in a quartz protection inside the quartz reactor. The flue gas was cooled and conducted to a condenser along with a liquid collector with tap, where the water and unreacted sulfuric acid were recovered. The gaseous products (SO_2 and O_2) were bubbled into a NaOH solution (6 M), where the SO_2 reacted producing sodium sulfite (Na_2SO_3), and the O_2 vented out.

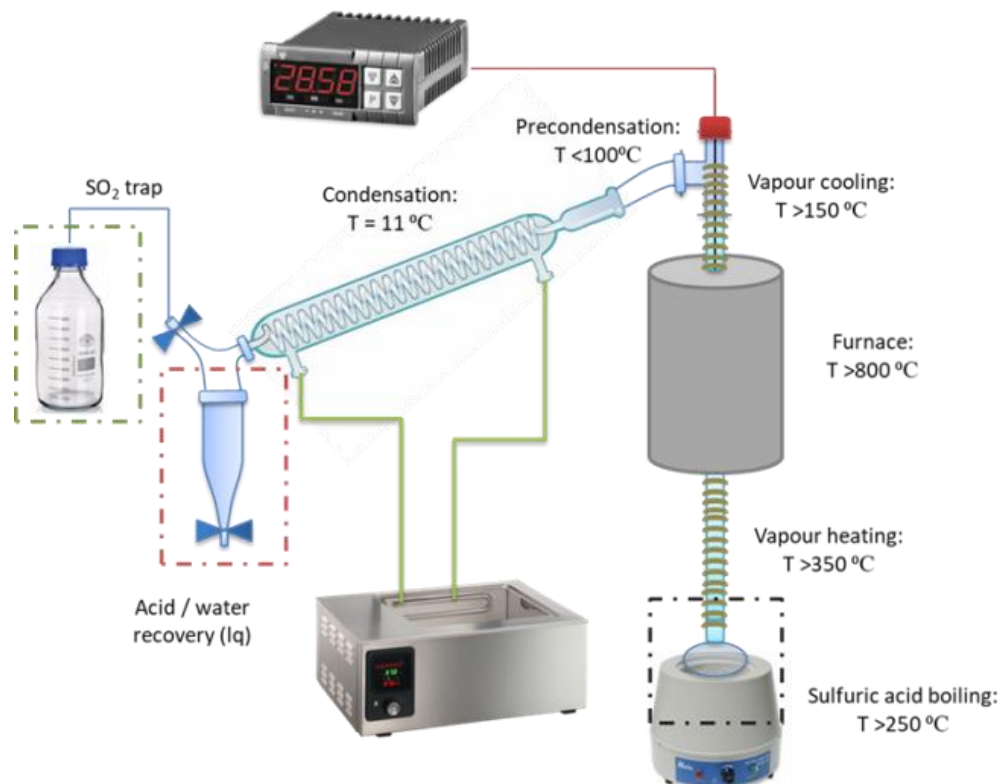
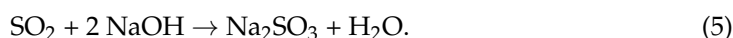


Figure 10. Experimental setup.

The condensed H_2SO_4 and the NaOH concentration in the trap were determined by titration using phenolphthalein as an indicator. The amount of SO_2 produced can be measured from the sulfite concentration in the trap, considering Reaction 5.



The sulfite concentration was determined by the iodate-iodide method. The sample was acidified and titrated with a potassium iodide-iodate solution (0.0125 N). Free iodine was released and reduced with sulfite to a colorless iodide. When all of the sulfite reacted, the sample acquired a blue color due to the iodine and starch indicator reaction.

The crystalline phases in the catalysts were analyzed by X-ray diffraction (XRD) using a Philips PW- 1700 diffractometer (Panalytical, Malvern, United Kingdom) with Cu K α radiation. Measurements of the 2 θ angle were located between 0 and 100° with a sweep speed of 0.02° min $^{-1}$. The morphology and surface composition of the catalyst were analyzed by scanning electron microscopy–energy dispersive X-ray spectroscopy (SEM-EDX) with a Microscope GeminiSEM 500 (ZEISS, Jena, Germany) at a 2 kV voltage with 10,000 \times magnification. The surface area of the catalysts was determined by N₂ adsorption at 77 K in an automated volumetric gas adsorption apparatus (Quantachrome Novatouch LX2, Odelzhausen, Germany). Previous to adsorption, the samples (0.15 g) were degassed under a vacuum at 323 K for 6 h. The Fourier transform infrared spectra (FTIR) were carried out on a Spectrum Two spectrometer (Perkin Elmer, Madrid, Spain) with a universal attenuated total reflectance (UATR) accessory. The samples were scanned from 4000 to 500 cm $^{-1}$ at a resolution of 16 cm $^{-1}$ at room temperature.

4. Conclusions

The main conclusion drawn from this work is that goethite can be used as a catalyst for the thermal decomposition of sulfuric acid in the Westinghouse cycle. Its activity is lower than that of Fe₂O₃ and CuO and higher than that of SiC. However, goethite does not undergo sintering during its use, but just produces small particles in its surface which remain after the treatment. Mixtures of Fe₂O₃ with SiC or goethite do not produce synergism, indicating that the action of each catalyst is not related to the other. In the future, long term experiments should be carried out to further know the activity and stability of goethite in its use as a catalyst of the Westinghouse process.

Author Contributions: Conceptualization, J.L. and M.A.R.; methodology, J.L. and M.A.R.; validation, J.L. and M.A.R.; investigation, C.M.F.-M., I.F.M. and A.R.; data curation, C.M.F.-M., I.F.M. and A.R.; writing—original draft preparation, C.M.F.-M., I.F.M. and A.R.; writing—review and editing, J.L. and M.A.R.; supervision, J.L. and M.A.R.; project administration, J.L. and M.A.R.; funding acquisition, J.L. and M.A.R. Frequent group meetings between the authors helped in analyzing and organizing the findings, until the final manuscript was obtained. All authors have read and agreed to the published version of the manuscript.

Funding: This research was funded by the Junta de Comunidades de Castilla-La Mancha and the FEDER EU Program, through the Project ASEPHAM, grant number “SBPLY/17/180501/000330”. Therefore, these Institutions are gratefully acknowledged. Ismael Fernández Mena is grateful to the Spanish Ministry of Science and Innovation for his postdoctoral fellowship, Juan de la Cierva Formación program (FJC2019-039962-I).

Conflicts of Interest: The authors declare no conflict of interest.

References

- Martino, M.; Ruocco, C.; Meloni, E.; Pullumbi, P.; Palma, V. Main hydrogen production processes: An overview. *Catalysts* **2021**, *11*, 547. [[CrossRef](#)]
- Khan, H.A.; Natarajan, P.; Jung, K.D. Stabilization of Pt at the inner wall of hollow spherical SiO₂ generated from Pt/hollow spherical SiC for sulfuric acid decomposition. *Appl. Catal. B Environ.* **2018**, *231*, 151–160. [[CrossRef](#)]
- Brecher, L.E.; Wu, C.K. Electrolytic Decomposition of Water. U.S. Patent No. 3,888,750, 10 June 1975.
- Brown, L.C.; Besenbruch, G.E.; Lentsch, R.D.; Schultz, K.R.; Funk, J.F.; Pickard, P.S.; Marshall, A.C.; Showalter, S.K. *High Efficiency Generation of Hydrogen Fuels Using Nuclear Power*; GA-A24285; General Atomics: San Diego, CA, USA, December 2003.
- Díaz-Abad, S.; Rodrigo, M.A.; Lobato, J. First approaches for hydrogen production by the depolarized electrolysis of SO₂ using phosphoric acid doped polybenzimidazole membranes. *Int. J. Hydrogen Energy* **2021**, *46*, 29763–29773. [[CrossRef](#)]
- Banerjee, A.M.; Pai, M.R.; Bhattacharya, K.; Tripathi, A.K.; Kamble, V.S.; Bharadwaj, S.R.; Kulshreshtha, S.K. Catalytic decomposition of sulfuric acid on mixed Cr/Fe oxide samples and its application in sulfur-iodine cycle for hydrogen production. *Int. J. Hydrogen Energy* **2008**, *33*, 319–326. [[CrossRef](#)]
- Wang, L.; Zhu, Y.; Yang, H.; He, Y.; Xia, J.; Zhang, Y.; Wang, Z. SO₃ decomposition over CuO–CeO₂ based catalysts in the sulfur-iodine cycle for hydrogen production. *Int. J. Hydrogen Energy* **2018**, *43*, 14876–14884. [[CrossRef](#)]
- Safari, F.; Dincer, I. A review and comparative evaluation of thermochemical water splitting cycles for hydrogen production. *Energy Convers. Manag.* **2020**, *205*, 112182. [[CrossRef](#)]

9. Díaz-Abad, S.; Millán, M.; Rodrigo, M.A.; Lobato, J. Review of anodic catalysts for SO₂ depolarized electrolysis for “green hydrogen” production. *Catalysts* **2019**, *9*, 63. [[CrossRef](#)]
10. Machida, M.; Ikematsu, A.; Nur, A.S.M.; Yoshida, H. Catalytic SO₃ Decomposition Activity of SiO₂-Supported Alkaline Earth Vanadates for Solar Thermochemical Water Splitting Cycles. *ACS Appl. Energy Mater.* **2021**, *4*, 1696–1703. [[CrossRef](#)]
11. Noh, S.C.; Lee, S.Y.; Shul, Y.G.; Jung, K.D. Sulfuric acid decomposition on the Pt/n-SiC catalyst for SI cycle to produce hydrogen. *Int. J. Hydrogen Energy* **2014**, *39*, 4181–4188. [[CrossRef](#)]
12. Rashkeev, S.N.; Ginosar, D.M.; Petkovic, L.M.; Farrell, H.H. Catalytic activity of supported metal particles for sulfuric acid decomposition reaction. *Catal. Today* **2009**, *139*, 291–298. [[CrossRef](#)]
13. Petkovic, L.M.; Ginosar, D.M.; Rollins, H.W.; Burch, K.C.; Pinhero, P.J.; Farrell, H.H. Pt/TiO₂ (rutile) catalysts for sulfuric acid decomposition in sulfur-based thermochemical water-splitting cycles. *Appl. Catal. A Gen.* **2008**, *338*, 27–36. [[CrossRef](#)]
14. Banerjee, A.M.; Pai, M.R.; Tewari, R.; Raje, N.; Tripathi, A.K.; Bharadwaj, S.R.; Das, D. A comprehensive study on Pt/Al₂O₃ granular catalyst used for sulfuric acid decomposition step in sulfur-iodine thermochemical cycle: Changes in catalyst structure, morphology and metal-support interaction. *Appl. Catal. B Environ.* **2015**, *162*, 327–337. [[CrossRef](#)]
15. Khan, H.A.; Iqbal, M.I.; Jaleel, A.; Abbas, I.; Abbas, S.A.; Deog-Jung, K. Pt encapsulated hollow mesoporous SiO₂ sphere catalyst for sulfuric acid decomposition reaction in SI cycle. *Int. J. Hydrogen Energy* **2019**, *44*, 2312–2322. [[CrossRef](#)]
16. Nur, A.S.M.; Matsukawa, T.; Hinokuma, S.; Machida, M. Catalytic SO₃ decomposition activity and stability of Pt supported on anatase TiO₂ for solar thermochemical water-splitting cycles. *ACS Omega* **2017**, *2*, 7057–7065. [[CrossRef](#)] [[PubMed](#)]
17. Ginosar, D.M.; Petkovic, L.M.; Glenn, A.W.; Burch, K.C. Stability of supported platinum sulfuric acid decomposition catalysts for use in thermochemical water splitting cycles. *Int. J. Hydrogen Energy* **2007**, *32*, 482–488. [[CrossRef](#)]
18. Zhang, P.; Su, T.; Chen, Q.H.; Wang, L.J.; Chen, S.Z.; Xu, J.M. Catalytic decomposition of sulfuric acid on composite oxides and Pt/SiC. *Int. J. Hydrogen Energy* **2012**, *37*, 760–764. [[CrossRef](#)]
19. Banerjee, A.M.; Shirole, A.R.; Pai, M.R.; Tripathi, A.K.; Bharadwaj, S.R.; Das, D.; Sinha, P.K. Catalytic activities of Fe₂O₃ and chromium doped Fe₂O₃ for sulfuric acid decomposition reaction in an integrated boiler, preheater, and catalytic decomposer. *Appl. Catal. B Environ.* **2012**, *127*, 36–46. [[CrossRef](#)]
20. Tagawa, H.; Endo, T. Catalytic decomposition of sulfuric acid using metal oxides as the oxygen generating reaction in thermochemical water splitting process. *Int. J. Hydrogen Energy* **1989**, *14*, 11–17. [[CrossRef](#)]
21. Ginosar, D.M.; Rollins, H.W.; Petkovic, L.M.; Burch, K.C.; Rush, M.J. High-temperature sulfuric acid decomposition over complex metal oxide catalysts. *Int. J. Hydrogen Energy* **2009**, *34*, 4065–4073. [[CrossRef](#)]
22. Nadar, A.; Banerjee, A.M.; Pai, M.R.; Pai, R.V.; Meena, S.S.; Tewari, R.; Tripathi, A.K. Catalytic properties of dispersed iron oxides Fe₂O₃/MO₂ (M = Zr, Ce, Ti and Si) for sulfuric acid decomposition reaction: Role of support. *Int. J. Hydrogen Energy* **2018**, *43*, 37–52. [[CrossRef](#)]
23. Lorenzo, D.; Dominguez, C.M.; Romero, A.; Santos, A. Wet peroxide oxidation of chlorobenzenes catalyzed by goethite and promoted by hydroxylamine. *Catalysts* **2019**, *9*, 553. [[CrossRef](#)]
24. Wu, J.; Zhao, X.; Li, Z.; Gu, X. Thermodynamic and kinetic coupling model of Cd(II) and Pb(II) adsorption and desorption on goethite. *Sci. Total Environ.* **2020**, *727*, 138730. [[CrossRef](#)]
25. Lorenzo, D.; Santos, A.; Sánchez-Yepes, A.; Conte, L.Ó.; Domínguez, C.M. Abatement of 1,2,4-trichlorobencene by wet peroxide oxidation catalysed by goethite and enhanced by visible led light at neutral ph. *Catalysts* **2021**, *11*, 139. [[CrossRef](#)]
26. Bae, D.; Seger, B.; Vesborg, P.C.K.; Hansen, O.; Chorkendorff, I. Strategies for stable water splitting: Via protected photoelectrodes. *Chem. Soc. Rev.* **2017**, *46*, 1933–1954. [[CrossRef](#)]
27. Ouachitak, H.; Akhouairi, S.; Haounati, R.; Addi, A.A.; Jada, A.; Taha, M.L.; Douch, J. 3,4-dihydroxybenzoic acid removal from water by goethite modified natural sand column fixed-bed: Experimental study and mathematical modeling. *Desalin. Water Treat.* **2020**, *194*, 439–449. [[CrossRef](#)]